

Magnetic subband structure of an electron on a triangular lattice

Gi-Yeong Oh*

Department of Basic Science, Hankyong National University,
Kyonggi-do 456-749, Korea
(submitted to Phys. Rev. B on June 29, 1999)

The effects of anisotropic nearest-neighbor (NN) and isotropic next-nearest-neighbor (NNN) hopping integrals on the magnetic subband structure of an electron on a triangular lattice are studied within the tight-binding approximation. A generalized Harper equation that includes both the NN and the NNN hopping terms is first derived. Then, the effects of anisotropic NN hopping integrals are examined and the results are compared in detail with those of an existing literature [Phys. Rev. B **56**, 3787 (1997)]. It is found that the hopping anisotropy generically leads to the occurrence of band broadening and gap closing. The effects of isotropic NNN hopping integrals are next examined, and it is found that introducing the NNN hopping integral changes considerably the magnetic subband structure; band broadening, gap closing, gap reopening, and band crossing occur depending on the strength of the isotropic NNN hopping integral. Symmetries of the magnetic subband structures with and without both the hopping anisotropy and the isotropic NNN hopping integrals are also discussed.

PACS numbers: 71.28.+d, 71.20.-b, 73.20.Dx, 71.45.Gm

I. INTRODUCTION

The problem of a two-dimensional (2D) Bloch electron under a perpendicular magnetic field has attracted much interest for several decades, since not only it exhibits extremely rich energy band structures^{1–7} but also it is closely related with various phenomena such as the quantum Hall effect,⁸ the flux-state model for high- T_c superconductivity,⁹ and the mean-field transition temperature of superconducting networks or Josephson junction arrays.¹⁰ Recently, by means of the remarkable advent of nanofabrication techniques, studies of finding the indication of the peculiar band structure and its effect on the transport and optical properties have been also extensively performed.^{11–14}

A traditional method to solve this problem is to start with energy dispersion $\varepsilon(\vec{k})$ without a magnetic field and then make the Peierls substitution $\vec{k} \rightarrow (\vec{p} + e\vec{A})/\hbar$ to construct an effective single-band Hamiltonian

$$H = \varepsilon[(\vec{p} + e\vec{A})/\hbar], \quad (1)$$

where \vec{p} is the momentum operator and \vec{A} is a vector potential. An equivalent way to this method is to start directly with the tight-binding Hamiltonian given by

$$H = \sum_{ij} t_{ij} e^{i\theta_{ij}} |i\rangle\langle j|, \quad (2)$$

where t_{ij} is the hopping integral between the sites i and j , $|i\rangle$ is a state of an atomiclike orbital centered at the site i , and θ_{ij} is the magnetic phase factor defined by

$$\theta_{ij} = \frac{2\pi}{\phi_0} \int_i^j \vec{A} \cdot d\vec{l}, \quad (3)$$

$\phi_0 = hc/e$ being the magnetic flux quantum.

So far, a number of works have focused on the energy spectrum of a lattice with a square symmetry, and the magnetic subband structure of the lattice with isotropic hopping integrals between nearest-neighbor (NN) sites is well known as the Hofstadter's butterfly.^{2,4} The effect of the anisotropy in the NN hopping integrals on the magnetic subband structure was also studied, and it was found that introducing the hopping anisotropy leads to the occurrence of band broadening and gap closing.^{15–18} Furthermore, the effect of next-nearest-neighbor (NNN) hopping integrals on the magnetic subband structure was also studied,¹⁹ and introducing the NNN hopping integrals was found to play a key role in removing the degeneracy which appears at the band center of the energy spectrum under isotropic NN hopping integrals.

Along with the case of the square lattice, magnetic subband structures of a triangular lattice have been intensively studied,^{16,20–24} and it was found that the lattice with isotropic NN hopping integrals exhibits a recursive magnetic subband structure similarly to the case of the square lattice with isotropic NN hopping integrals.²¹ Recently, the effect of the anisotropy in the NN hopping integrals on the magnetic subband structure was studied by Gumbs and Fekete.²⁴ In studying the effect, they applied the Peierls substitution for the energy dispersion given by

$$\varepsilon(\vec{k}) = 2 \left\{ t_a \cos(k_x a) + t_b \cos \left[(k_x + \sqrt{3}k_y) \frac{a}{2} \right] \right. \\ \left. + t_c \cos \left[(k_x - \sqrt{3}k_y) \frac{a}{2} \right] \right\} \quad (4)$$

to construct a Hamiltonian matrix. And, by diagonalizing the resultant matrix, they obtained magnetic subband structures for a few sets of (t_a, t_b, t_c) and presented relevant arguments. However, unfortunately, most of the

results and arguments presented by them are erroneous ones that arise from a mistake in deriving the Hamiltonian, as we shall show below. We re-examine the same problem as that investigated by Gumbs and Fekete to put the correct formalism and numerical results, which is the first end of this paper. The second end of this paper is to examine the effect of isotropic NNN hopping integrals on the magnetic subband structure. To our knowledge, few work has been devoted to this problem. However, noting that the triangular lattice with NNN hopping integrals is topologically equivalent to the square lattice with NNN hopping integrals, it may be interesting to examine this problem and compare the results with the case of the square lattice. We will show that the magnetic subband structure changes considerably depending on the strength of the isotropic NNN hopping integrals.

This paper is organized as follows: In Sec. II, we derive a generalized Harper equation that includes NNN as well as NN hopping integrals. In Sec. III, we first point out the mistake and the misleading arguments presented in Ref. 24, and then present correct numerical results on the effects of both anisotropic NN and isotropic NNN hopping integrals on the magnetic subband structure. We also discuss the symmetries of the magnetic subband structure obtained from the generalized Harper equation. Finally, Sec. IV is devoted to a brief summary.

II. THE TIGHT-BIDING EQUATION

We consider an electron on a 2D triangular lattice with a hexagonal symmetry in the presence of a uniform perpendicular magnetic field $\vec{B} = B\hat{z}$. Under the Landau gauge, the vector potential is given by $\vec{A} = (0, Bx, 0)$ and θ_{ij} is given by

$$\theta_{ij} = \begin{cases} 0, & j = (m \pm 2, n) \\ \pm\pi\phi(m \pm 1/2), & j = (m \pm 1, n \pm 1) \\ \pm\pi\phi(m \mp 1/2), & j = (m \mp 1, n \pm 1) \\ \pm\pi\phi(m \pm 3/2), & j = (m \pm 3, n \pm 1) \\ \pm\pi\phi(m \mp 3/2), & j = (m \mp 3, n \pm 1) \\ \pm 2\pi\phi m, & j = (m, n \pm 2) \end{cases}, \quad (5)$$

where $i = (m, n)$. Here, (m, n) labels the lattice points, i.e., $(x, y) = (mb, nc)$, where $b = a/2$, $c = \sqrt{3}a/2$, and a is the lattice constant. And, $\phi = 2\sqrt{3}Bb^2/\phi_0$ is the magnetic flux through the unit cell. By means of Eqs. (2)

$$\mathbf{A} = \begin{pmatrix} A_1 & B_1 & t_a & C_2 & \dots & C_{M-1}^* e^{-i\delta} & t_a e^{-i\delta} & B_M^* e^{-i\delta} \\ B_1^* & A_2 & B_2 & t_a & \dots & 0 & C_M^* e^{-i\delta} & t_a e^{-i\delta} \\ t_a & B_2^* & A_3 & B_3 & \dots & 0 & 0 & C_1^* e^{-i\delta} \\ C_2^* & t_a & B_3^* & A_4 & \dots & 0 & 0 & 0 \\ \vdots & \vdots & \vdots & \vdots & \ddots & \vdots & \vdots & \vdots \\ C_{M-1} e^{i\delta} & 0 & 0 & 0 & \dots & A_{M-2} & B_{M-2} & t_a \\ t_a e^{i\delta} & C_M e^{i\delta} & 0 & 0 & \dots & B_{M-2}^* & A_{M-1} & B_{M-1} \\ B_M e^{i\delta} & t_a e^{i\delta} & C_1 e^{i\delta} & 0 & \dots & t_a & B_{M-1}^* & A_M \end{pmatrix} \quad (12)$$

and (5), the tight-binding equation, $H\Psi_{m,n} = E\Psi_{m,n}$, can be written as

$$\begin{aligned} E\Psi_{m,n} = & t_a(\Psi_{m-2,n} + \Psi_{m+2,n}) \\ & + t_b[e^{i\pi\phi(m-1/2)}\Psi_{m-1,n-1} + e^{-i\pi\phi(m+1/2)}\Psi_{m+1,n+1}] \\ & + t_c[e^{i\pi\phi(m+1/2)}\Psi_{m+1,n-1} + e^{-i\pi\phi(m-1/2)}\Psi_{m-1,n+1}] \\ & + t'_a[e^{i\pi\phi(m-3/2)}\Psi_{m-3,n-1} + e^{-i\pi\phi(m+3/2)}\Psi_{m+3,n+1}] \\ & + t'_c[e^{i\pi\phi(m+3/2)}\Psi_{m+3,n-1} + e^{-i\pi\phi(m-3/2)}\Psi_{m-3,n+1}] \\ & + t'_b(e^{i2\pi\phi m}\Psi_{m,n-2} + e^{-i2\pi\phi m}\Psi_{m,n+2}), \end{aligned} \quad (6)$$

where t_a is the NN hopping integral along the x direction, $t_{b(c)}$ is the NN hopping integral along the direction which makes $\pi/3$ ($2\pi/3$) with the x direction, and $t'_{a(b,c)}$ is the NNN hopping integral along the direction which makes $\pi/6$ ($\pi/2$, $5\pi/6$) with the x direction, respectively.

Since Eq. (6) is invariant under the transformation $y \rightarrow y + \sqrt{3}a$, $\Psi_{m,n}$ can be written as

$$\Psi_{m,n} = e^{i\sqrt{3}k_y n a} \psi_m. \quad (7)$$

Thus, using Eqs. (6) and (7), we obtain a kind of generalized Harper equation as follows:

$$\begin{aligned} E\psi_m = & C_{m-2}^* \psi_{m-3} + t_a \psi_{m-2} + B_{m-1}^* \psi_{m-1} + A_m \psi_m \\ & + B_m \psi_{m+1} + t_a \psi_{m+2} + C_{m+1} \psi_{m+3}, \end{aligned} \quad (8)$$

where

$$\begin{aligned} A_m &= 2t'_b \cos(2\theta_m - \pi\phi), \\ B_m &= t_c e^{i\theta_m} + t_b e^{-i\theta_m}, \\ C_m &= t'_c e^{i\theta_m} + t'_a e^{-i\theta_m}, \end{aligned} \quad (9)$$

with $\theta_m = \pi\phi(m - 1/2) - k_y c$. Denoting $\phi = p/q$ with relative primes p and q , it can be easily checked that

$$A_{m+q} = A_m, \quad B_{m+M} = B_m, \quad C_{m+M} = C_m, \quad (10)$$

where $M = q$ ($2q$) for an even (odd) p . Thus, m in Eq. (8) satisfies the condition $1 \leq m \leq q$ ($1 \leq m \leq 2q$) for an even (odd) p , and the Bloch condition along the x direction can be written as

$$\psi_{m+M} = e^{ik_x M b} \psi_m. \quad (11)$$

Using Eqs. (8) and (11), we obtain the eigenvalue equation, $\mathbf{A}\Psi = E\Psi$, where $\Psi^\dagger = (\psi_1, \psi_2, \dots, \psi_M)$ and

with $\delta = k_x qa/2$ ($k_x qa$) for an even (odd) p .

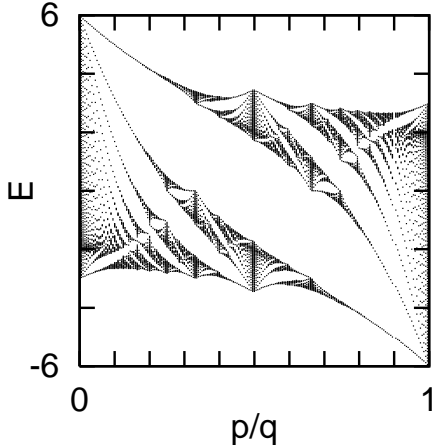


FIG. 1. Energy eigenvalues versus ϕ for a triangular lattice with isotropic NN hopping integrals ($t_a = t_b = t_c = 1$). Calculations are performed for $\phi = p/199$ with $1 \leq p \leq 198$, and the central value of \vec{k} in the MBZ is taken into account.

III. NUMERICAL RESULTS AND DISCUSSION

Before presenting our numerical results, we would like to point out the mistake made by Gumbs and Fekete in Ref. 24. In converting Eq. (4) into Eq. (1) [i.e., Eq. (2) of Ref. 24], they made a mistake in operating $e^{\pm i(p_x \pm \sqrt{3}eBx)a/2\hbar}$ to $\Psi_{m,n}$. According to them, the results of the operations are given by

$$\begin{aligned} e^{\pm i(p_x + \sqrt{3}eBx)a/2\hbar} \Psi_{m,n} &= e^{\pm i\pi\phi m} \Psi_{m \mp 1, n}, \\ e^{\pm i(p_x - \sqrt{3}eBx)a/2\hbar} \Psi_{m,n} &= e^{\mp i\pi\phi m} \Psi_{m \mp 1, n}. \end{aligned} \quad (13)$$

However, these are incorrect since the fundamental commutation relation $[x, p_x] = i\hbar$ is ignored in the operation. The correct results taking into account this relation should be expressed as²⁵

$$\begin{aligned} e^{\pm i(p_x + \sqrt{3}eBx)a/2\hbar} \Psi_{m,n} &= e^{\pm i\pi\phi(m \mp 1/2)} \Psi_{m \mp 1, n}, \\ e^{\pm i(p_x - \sqrt{3}eBx)a/2\hbar} \Psi_{m,n} &= e^{\mp i\pi\phi(m \mp 1/2)} \Psi_{m \mp 1, n}. \end{aligned} \quad (14)$$

We can easily check that the same equation as Eq. (6) with $t'_a = t'_b = t'_c = 0$ can be obtained by the method of the Peierls substitution if Eq. (14) instead of Eq. (13) is applied. In fact, Eq. (6) of Ref. 24, which was derived by means of Eq. (13), is a non-Hermitian matrix, and thus it is unreasonable to obtain real energy eigenvalues from this matrix.

Figure 1 shows the $E - \phi$ diagram obtained by diagonalizing Eq. (12) for the parameters $t_a = t_b = t_c = 1$, $\vec{k} = 0$, and $\phi = p/199$ with $1 \leq p \leq 198$ in the absence of the NNN hopping integral ($t'_a = t'_b = t'_c = 0$). It is obvious that the energy spectrum is *not* symmetric about $\phi = 1/2$ and there is *no* distinct array of energy eigenvalues parallel to the energy axis in the two largest energy gaps, contrary to the argument of Gumbs and Fekete [see

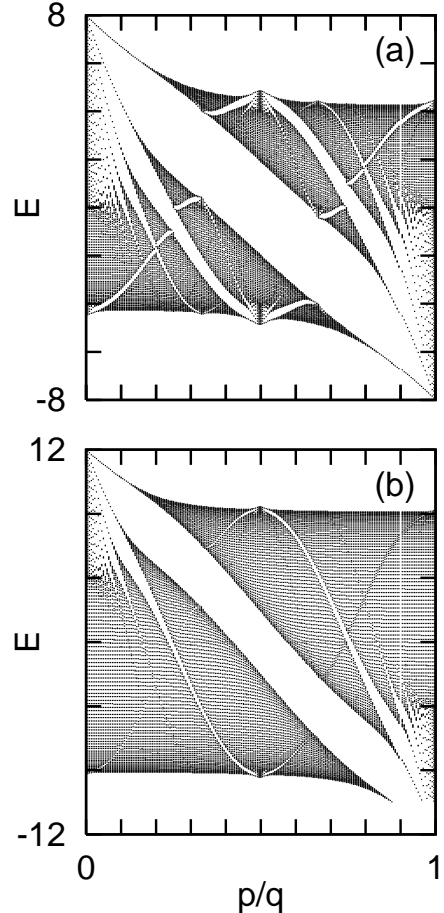


FIG. 2. Energy eigenvalues versus ϕ for a lattice with (a) $(t_a, t_b, t_c) = (2, 1, 1)$ and (b) $(t_a, t_b, t_c) = (4, 1, 1)$. Other parameters are the same as Fig. 1.

Fig. 1 and the relevant arguments of Ref. 24]. In fact, Fig. 1 of this paper is exactly the same as Fig. 3 of Ref. 21 presented by Claro and Wannier if E is replaced by $-(E - \epsilon_0)/2\epsilon_1$, which is quite natural because both of the two papers deal with the same problem. The only difference between the two papers lies in choosing the x and y directions; the axes taken in Ref. 21 are turned by $\pi/6$ from those in this paper. Note that, even though the choice of the axes in Ref. 21 yields a three-term difference equation [see Eq. (10) of Ref. 21] while the choice in this paper yields a five-term difference equation in the absence of NNN hopping integrals, the resultant energy band structures are the same, as shown above.

A. Effects of anisotropic NN hopping integrals

Figure 2 is the $E - \phi$ diagram for the parameters $t_b = t_c = 1$, $\vec{k} = 0$, and (a) $t_a = 2$ and (b) $t_a = 4$ in the absence of NNN hopping integrals. The increase of

total bandwidths and the occurrence of gap closing except for a few large ones are clearly seen. We argue that these behaviors may be generic effects of the hopping anisotropy, since the same phenomena were also observed in the square lattice.^{16–18} Note that Fig. 3 of Ref. 24 is the $E - \phi$ diagram plotted for the same parameters used in plotting Fig. 2(a) of this paper, from which Gumbs and Fekete argued that the bottom of the energy band is very flat near $E = -4$ and that the spectrum is symmetric about $\phi = 1/2$. However, it is evident that their arguments are incorrect. In regard to Figs. 2 – 4 of Ref. 24, we would like to point out that the $E - \phi$ diagrams for the parameters $(t_a, t_b, t_c) = (1, 2, 1), (2, 1, 1)$, and $(1, 1, 2)$ should be exactly the same when all the values of \vec{k} in the magnetic Brillouin zone (MBZ; $|k_x| \leq 2\pi/Ma$ and $|k_y| \leq \pi/\sqrt{3}a$) are taken into account, which means that there is no preferable direction in the lattice plane under a uniform perpendicular magnetic field.

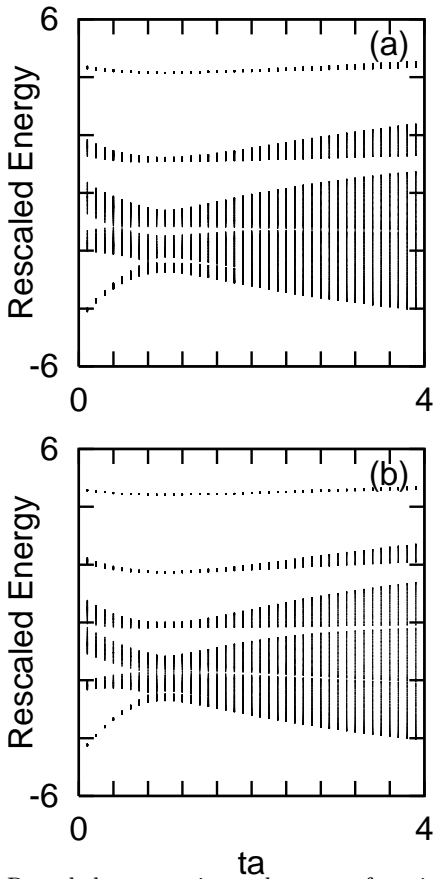


FIG. 3. Rescaled energy eigenvalues as a function of t_a for a lattice with (a) $\phi = 1/5$ and (b) $\phi = 1/6$, and $t_b = t_c = 1$. All the values of \vec{k} in the MBZ are taken into account.

In order to get more information on the anisotropy dependence of the subgap widths, we calculate the band structure as a function of the hopping anisotropy. Note that the energy eigenvalues in the absence of a magnetic field satisfy the condition $|\varepsilon(\vec{k})| \leq 2(t_a + t_b + t_c)$ [see Eq. (4)] and the total bandwidth increases linearly with

the increase of t_a . Assuming the situation also holds in the presence of a uniform magnetic field, we can introduce the rescaled energy defined by

$$E_{re} = 3E/(t_a + t_b + t_c). \quad (15)$$

Then, E_{re} is always in the range of $[-6, 6]$ regardless of the strength of the hopping anisotropy, and we can examine more clearly the dependence of the subgap widths on the hopping anisotropy, in comparison with the isotropic case.

Figure 3(a) shows the t_a dependence of the band structure for $\phi = 1/5$, where $t_b = t_c = 1$ and all the values of \vec{k} in the MBZ are taken into account. At isotropic case ($t_a = 1$), there are five subbands and four subgaps. However, introducing the hopping anisotropy ($t_a \neq 1$) changes the band structure considerably. Let us number the subgaps from the bottom of the energy spectrum. Then, in the regime of $t_a > 1$, the first and the second subgaps close for a small amount of anisotropy, while the third and the fourth subgaps survive even for large values of anisotropy. However, since the widths of the third and the fourth subgaps decrease with increasing t_a , we expect that these subgaps will also close in the limit of $t_a \rightarrow \infty$. And, in the regime of $t_a < 1$, the widths of the third and the fourth subgaps decrease with decreasing t_a , as in the case of $t_a > 1$. Meanwhile, the first and the second subgaps exhibit an interesting behavior. As t_a decreases, the width of the first (second) subgap decreases such that it closes at $t_a \simeq 0.8$ ($t_a \simeq 0.45$). And, as t_a decreases further, the subgap reopens and its width increases such that the width of the first (second) subgap becomes the same as that of the fourth (third) subgap, resulting in a symmetric band structure about $E = 0$ in the limit of $t_a \rightarrow 0$. Since the triangular lattice with the parameters $(t_a, t_b, t_c) = (0, 1, 1)$ is topologically equivalent to the square lattice with isotropic NN hopping integrals, it is natural of the band structure to be symmetric about $E = 0$.

As an another example, we plot in Fig. 3(b) the t_a dependence of the band structure for $\phi = 1/6$. At isotropic case ($t_a = 1$), there might be six subbands and five subgaps. However, due to the occurrence of band touching between the second and the third subbands, the second subgap is missing and the energy spectrum consists of four subgaps. And, in the regime of $t_a > 1$, we observe that the first subgap close even for a small amount of anisotropy and the third subgap close for a large value of anisotropy. Besides, since the widths of the fourth and the fifth subgaps decrease with increasing t_a , the closing of these subgaps is expected in the limit of $t_a \rightarrow \infty$. Meanwhile, the t_a dependence of the missing second subgap exhibits an interesting feature; the subgap opens with increasing t_a , even though its width is very small. In the regime of $t_a < 1$, we can see that the width of the first (second) subgap increases with decreasing t_a such that the width becomes the same as that of the fifth (fourth) subgap, resulting in a symmetric band structure

about $E = 0$ in the limit of $t_a \rightarrow 0$. And, the width of the third subgap decreases with decreasing t_a and closes at $t_a = 0$. Thus, there occurs a degeneracy at the band

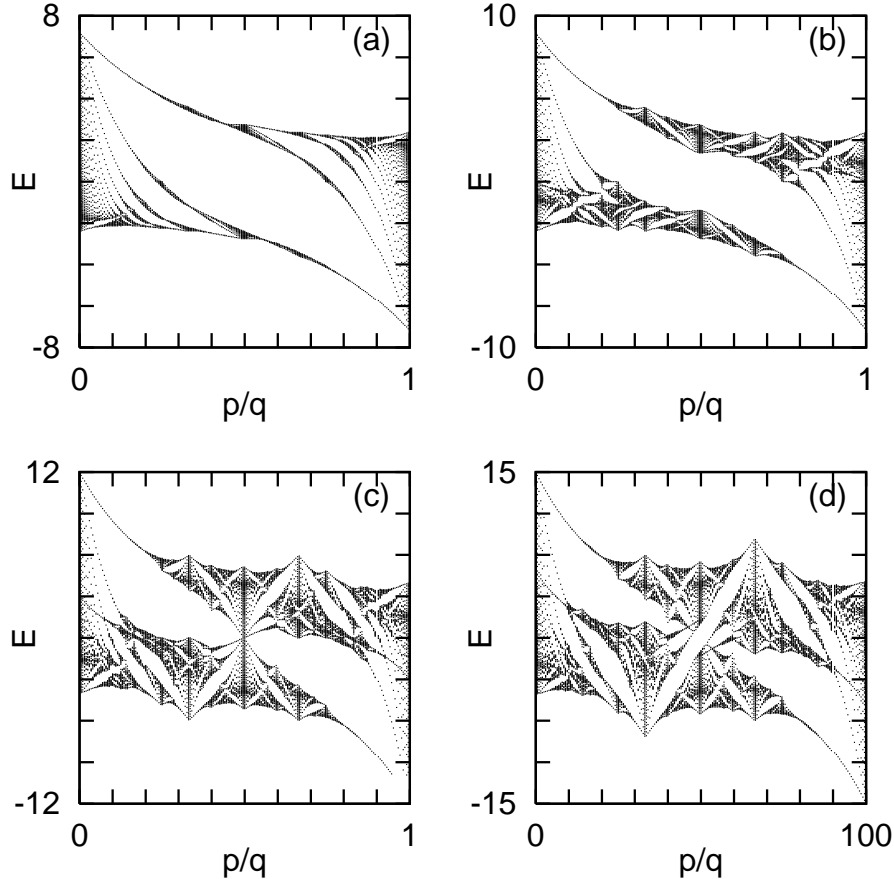


FIG. 4. Energy eigenvalues versus ϕ for a lattice with (a) $t' = 0.2$, (b) $t' = 0.5$, (c) $t' = 1.0$, and (d) $t' = 1.2$, respectively. Other parameters are the same as Fig. 1.

B. Effects of isotropic NNN hopping integrals

In calculating energy eigenvalues with varying the NNN hopping integrals, we set $t_a = t_b = t_c = 1$ and assume that the NNN hopping integrals are isotropic, i.e., $t'_a = t'_b = t'_c (\equiv t')$. Figure 4 shows the $E - \phi$ diagram for (a) $t' = 0.2$, (b) $t' = 0.5$, (c) $t' = 1.0$, and (d) $t' = 1.2$, respectively. We can see that the fractal structure in the energy spectrum appears despite of introducing the NNN hopping integral, which may attribute to the isotropy of the NN and the NNN hopping integrals. We can also see that, even though the total bandwidths for $\phi = 0$ and 1 increase monotonically with increasing t' , the bandwidths for generic values of ϕ depend crucially on t' , resulting in diverse shapes of $E - \phi$ diagrams. For small values of t' , the bandwidths become narrower than the case of $t' = 0$ and the resultant diagram exhibits a very narrow structure [see Fig. 4(a)]. However, the bandwidths increase with increasing t' , resulting in a fat structure of $E - \phi$ diagram [see Figs. 4(b) - 4(d)].

Figure 5 shows the t' dependence of the band struc-

center of the energy spectrum, as in the case of the square lattice with isotropic NN hopping integrals.

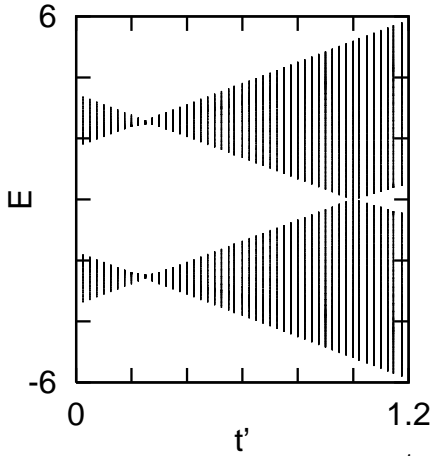


FIG. 5. Energy eigenvalues as a function of t' for a lattice with $\phi = 1/2$. All the values of \vec{k} in the MBZ are taken into account.

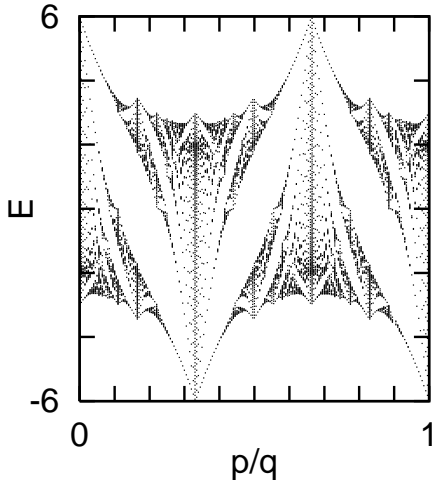


FIG. 6. Energy eigenvalues versus ϕ for a lattice with $t = 0$ and $t' = 1$. The data are obtained for $\phi = p/199$ with $1 \leq p \leq 198$ and for $\vec{k} = 0$.

t' such that $E_l(\phi = 1/3) = E_l(\phi = 1)$ [$E_h(\phi = 2/3) = E_h(\phi = 0)$] in the limit of $t'/t \rightarrow \infty$, where $E_{l(h)}$ means the lowest (highest) subband edge. From this behavior, it can be expected that the periodicity of the $E - \phi$ diagram in the limit of $t'/t \rightarrow \infty$ reduces by three times in ϕ . Figure 6 shows the $E - \phi$ diagrams for the lattice with $t = 0$ and $t' = 1$, which confirms this expectation. Note that it is nothing but an energy spectrum for the lattice with the isotropic hopping integral ($t' = 1$) and the lattice constant $\sqrt{3}a$. In order to see the t' dependence of the band structure for generic values of ϕ , we plot in Fig. 7 the $E - t'$ diagrams for (a) $\phi = 1/7$ and (b) $\phi = 2/7$. We can see that gap closing, gap reopening, and band crossing occur depending on the values of t' .

Before concluding this section, we discuss the symmetry of the energy spectrum. Denoting the set of energy eigenvalues for a wave vector \vec{k} under a flux ϕ as $E(\phi; \vec{k})$ and the energy spectrum taking into account all the val-

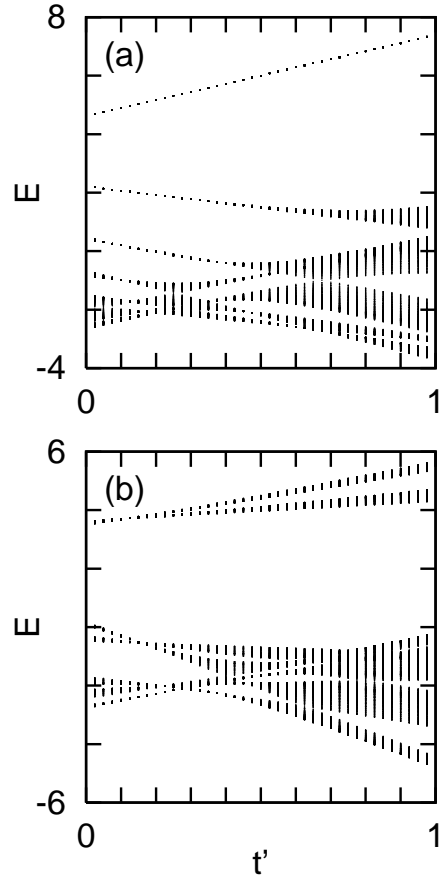


FIG. 7. Energy eigenvalues as a function of t' for a lattice with (a) $\phi = 1/7$ and (b) $\phi = 2/7$. All the values of \vec{k} in the MBZ are taken into account.

ues of \vec{k} in the MBZ as $E(\phi)$, we can see the following properties of the band structure for generic values of NN hopping integrals: (i) $E(\phi; \vec{k}) = E(\phi; -\vec{k})$, (ii) $E(\phi) = E(-\phi)$, (iii) $E(\phi) = -E(1-\phi)$ with $0 \leq \phi \leq 1/2$, and (iv) $E(\phi) = E(\phi+2)$. Note that the property (i) can be easily checked in Eq. (12); $\mathbf{A} \rightarrow \mathbf{A}^\dagger$ under the transformation $\vec{k} \rightarrow -\vec{k}$. Note also that the property (ii) means that there is no way for an electron to discern the direction of the magnetic field. Figures 1 and 2 show that the properties (iii) and (iv) hold in the presence of the NN hopping anisotropy. And, Fig. 4 also shows that the properties (i)–(iv) hold in the presence of NNN hopping integrals except for the case of $t = 0$; when $t = 0$, the properties (iii) and (iv) are replaced by $E(\phi) = -E(1/3 - \phi)$ with $0 \leq \phi \leq 1/6$ and $E(\phi) = E(\phi + 2/3)$, respectively, as can be seen in Fig. 6.

IV. SUMMARY

In summary, the effects of anisotropic NN hopping integrals and of isotropic NNN hopping integrals on the magnetic subband structure of an electron on a triangular lattice were studied within the tight-binding approximation. It was found that the phenomena of bandwidth

broadening, gap closing, and gap opening are generic feature of introducing the NN hopping anisotropy. It was also found that the magnetic subband structure changes considerably by introducing the NNN hopping integrals; bandwidth broadening, gap closing, gap reopening, and band crossing occur depending on the strength of the isotropic NNN hopping integrals. In the study, the dependence of the subgap widths on the hopping anisotropy and the NNN hopping integrals was illustrated in detail, and the symmetries of the magnetic subband structures with and without the hopping anisotropy and the NNN hopping integrals were also discussed. In order to deepen the understanding on the band structure of the triangular lattice, a further study of the effect of, for example, nonuniform magnetic fields²⁶ and an interaction between electrons²⁷ on the magnetic subband structure of the lattice is required, and the work is on doing.

ACKNOWLEDGMENTS

The author is grateful to Dr. J. Chung and Mrs. B. K. Min for stimulating discussions.

* Electronic address: ogy@hnu.hankyong.ac.kr

- ¹ R. Peierls, Z. Phys. **80**, 763 (1933); P. G. Harper, Proc. Phys. Soc. London A **68**, 874 (1955); W. Kohn, Phys. Rev. **115**, 1460 (1959); M. Ya Azbel, Zh. Éksp. Teor. Fiz. **46**, 929 (1994) [Sov. Phys. JETP **19**, 634 (1964)].
- ² D. R. Hofstadter, Phys. Rev. B **14**, 2239 (1976).
- ³ G. H. Wannier, Phys. Status Solidi B **88**, 757 (1978); G. H. Wannier, G. M. Obermaier, and R. Ray, *ibid.* **93**, 337 (1979).
- ⁴ A. H. MacDonald, Phys. Rev. B **28**, 6713 (1983).
- ⁵ J. B. Sokoloff, Phys. Rep. **126**, 189 (1985).
- ⁶ M-C. Chang and Q. Niu, Phys. Rev. B **53**, 7010 (1996).
- ⁷ Y. Hatsugai, M. Kohmoto, and Y-S. Wu, Phys. Rev. B **53**, 9697 (1996).
- ⁸ D. J. Thouless, M. Kohmoto, P. Nightingale, and M. Den Nijs, Phys. Rev. Lett. **49**, 405 (1982); R. Rammal, G. Toulouse, M. T. Jaekel, and B. I. Halperin, Phys. Rev. B **27**, 5142 (1983).
- ⁹ P. W. Anderson, Phys. Scr. T **27**, 60 (1989); P. Lederer, D. Poilblanc, and T. M. Rice, Phys. Rev. Lett. **63**, 1519 (1989).
- ¹⁰ S. Alexander, Phys. Rev. B **27**, 1541 (1983); R. Rammal, T. C. Lubensky and G. Toulouse, *ibid.* **27**, 2820 (1983); Q. Niu and F. Nori, *ibid.* **39**, 2134 (1989).
- ¹¹ B. Pannetier, J. Chaussy, R. Rammal, and J-C. Villegier, Phys. Rev. Lett. **53**, 1845 (1984).
- ¹² D. Weiss, M. L. Roukes, A. Menshig, P. Grambow, K. von Klitzing, and G. Wieman, Phys. Rev. Lett. **66**, 2790 (1991).
- ¹³ A. Lorke, J. P. Kotthaus, and K. Ploog, Phys. Rev. B **44**, 3447 (1991).
- ¹⁴ R. R. Gerhardts, D. Weiss, and U. Wulf, Phys. Rev. B **43**, 5192 (1991); R. R. Gerhardts and D. Pfannkuche, Surf. Sci. **263**, 324 (1992).
- ¹⁵ M. Kohmoto, Phys. Rev. B **39**, 11943 (1989).
- ¹⁶ Y. Hasegawa, Y. Hatsugai, M. Kohmoto, and G. Montambaux, Phys. Rev. B **41**, 9174 (1990).
- ¹⁷ S. N. Sun and J. P. Ralston, Phys. Rev. B **44**, 13603 (1991).
- ¹⁸ G. Y. Oh, J. Jang, and M. H. Lee, J. Korean Phys. Soc. **29**, 261 (1996).
- ¹⁹ Y. Hatsugai and M. Kohmoto, Phys. Rev. B **42**, 8282 (1990); J. H. Han, D. J. Thouless, H. Hiramoto, and M. Kohmoto, Phys. Rev. B **50**, 11365 (1994).
- ²⁰ D. Langbein, Phys. Rev. **180**, 633 (1969).
- ²¹ F. H. Claro and G. H. Wannier, Phys. Rev. B **19**, 6068 (1979).
- ²² D. J. Thouless, Phys. Rev. B **28**, 4272 (1983).
- ²³ O. Kühn, P. E. Shlbmann, V. Fessatidis, and H. L. Cui, J. Phys.: Condens. Matter **5**, 8225 (1993).
- ²⁴ G. Gumbs and P. Fekete, Phys. Rev. B **56**, 3787 (1997).
- ²⁵ S. Gasiorowicz, *Quantum Physics* (John Wiley & Sons Inc., 1974), p. 137.
- ²⁶ A. Barelli, J. Bellissard, and R. Rammal, J. Phys. (Paris) **51**, 2167 (1990); G. Y. Oh and M. H. Lee, Phys. Rev. B **53**, 1225 (1996); Q. W. Shi and K. Y. Szeto, *ibid.* **56**, 9251 (1997); G. Y. Oh, *ibid.* **60** (in press).
- ²⁷ H. Doh and S-H. Suck Salk, Phys. Rev. B **57**, 1312 (1998).